Fish and Shellfish Immunology 93 (2019) 508–516

Contents lists available at ScienceDirect

Fish and Shellfish Immunology

journal homepage: www.elsevier.com/locate/fsi

Full length article

Characterization of a new *il-4/13* homologue in grass carp (*Ctenopharyngodon idella*) and its cooperation with M-CSF to promote macrophage proliferation

Kun Yang*, Shiyu Feng, Shengnan Zhang, Licheng Yin, Hong Zhou, Anying Zhang, Xinyan Wang

Center for Informational Biology, School of Life Science and Technology, University of Electronic Science and Technology of China, Chengdu, People's Republic of China

ARTICLE INFO

Keywords:
Grass carp
IL-4/13b-like gene
M-csf
Arginase
Monocytes/macrophages
Proliferation

ABSTRACT

In this study, a new *il-4/13* cDNA was isolated from grass carp *(Ctenopharyngodon idella)* using homologous cloning. The phylogenetic tree and sequence alignment of the deduced amino acid (aa) sequence showed that it was closer to grass carp *il-4/13b* (*gcil-4/13b*) than other homologues and therefore named *gcil-4/13b-like* (*gcil-4/*13bl). It has 399-nt coding sequence (CDS) which is less than *gcil-4/13b* (408 nt). In addition, the cloned *gcil-4/*13bl gene is approximately 1600 bp in length and has a conserved genetic structure consisting of four exons and three introns. Compared to *gcil-4/13b* gene, it has a variety of nucleotides variation across the CDS and contains a longer intron 3, suggesting that it is a new *gcil-4/13* gene. The *gcil-4*/13bl transcripts were ubiquitously expressed in almost all selected tissues, and there was almost only *gcil-4*/13bl detected in brain and head kidney (HK). Recombinant grass carp (rgc) Il-4/13bl was prepared by using *Escherichia coli* (*E. coli*) Rosetta-gami 2 (DE3). The functional study demonstrated that rgcIl-4/13bl significantly upregulated *arginase-2* gene expression and arginase activity, whilst downregulated nitric oxide (NO) production as well as the transcript levels of inducible nitric oxide synthesase (*inos*) and *ifn*-γ in freshly isolated grass carp HK monocytes/macrophages (M0/Mϕ). These data suggested that the newly cloned *il-4*/13bl had the conserved functions to activate M2-type but antagonize M1-type macrophages. Furthermore, rgcIl-4/13bl was able to drive the proliferation of M0/Mϕ which were pre-treated by rgcM-csf, indicating the involvement of gcIl-4/13bl in the proliferation of macrophages. Here we not only identified a new *il-4/13*-encoding gene in grass carp, but also for the first time revealed a novel function of fish Il-4/13 combined with M-csf engaging in M0/Mϕ proliferation.

1. Introduction

IL-4 and IL-13 are two closely related cytokines. They both form a tertiary structure with “up-up-down-down” four alpha-helixes bundle, which is the characteristic of short chain type I cytokine, despite their low identity in protein sequences (~23%) [1]. In mammals, IL-4 and IL-13 are encoded by two single-copy genes respectively, and locate side by side between two conserved genes KIF3A (tail-to-tail) and RAD50 (head-to-tail) in the genome [2]. Both IL-4 and IL-13 are known for their ability to modulate adaptive immune responses in mammals, including activation of naive $CD4^+$ T cells to form type 2 T helper (Th2) cells, and induction of immunoglobulin production and class switching in B cells [3]. In addition, IL-4 up-regulates arginase and down-regulates iNOS expression, which catalize the same substrate, L-arginine, to antagonize the classically activated M1-type while alternatively activate M2-type macrophages, which play roles in wound healing, tissue repair and anti-sepsis [4].

There are two *il-4/13* loci found in the majority of fish species. The fish *il-4/13* loci are thought to have been amplified due to some events such as gene replication and genome replication from single-copy gene of ancestral spotted gar [2]. The two *il-4/13* homologues in fish are ambiguously phylogenetic related with mammalian IL-4 and IL-13 due to their very low degree of sequence similarities, and therefore named *il-4/13a* and *il-4/13b* [5,6]. However, analysis of fish genomes reveal a well conserved gene synteny at the KIF3A/RAD50 locus with mammalian counterparts. Therefore, the identification of *il-4/13a* and *il-4/13b* genes in several fish are usually facilitated by sequence alignment and gene localization based on genomic databases [5–7]. Several studies have shown that the functions of Il-4/13a and Il-4/13b are similar. For example, *in vivo* injection of recombinant tiger puffer Il-4/13a and

* Corresponding author. School of Life Science and Technology, University of Electronic Science and Technology of China, Chengdu, 610054, People's Republic of China.

E-mail address: yk_36_angel@uestc.edu.cn (K. Yang).

https://doi.org/10.1016/j.fsi.2019.07.070
Received 13 May 2019; Received in revised form 16 July 2019; Accepted 24 July 2019
Available online 26 July 2019

Il-4/13b proteins lead to the up-regulation of Il-6 and Il-12p40 [8]. In particular, upregulation of arginase II activity and/or mRNA levels in M0/Mϕ and down-regulation of *inos* expression and/or NO production are confirmed in rainbow trout [9], goldfish [10], grass carp [7] and large yellow croaker [11], showing the common functional features of fish Il-4/13.

In this study, we cloned a new *il-4/13* gene from grass carp by homologous cloning instead of database alignment. Phylogenetic tree and sequence alignment analysis showed that it was closer to *gcil-4/13b* [7] and was therefore nominated as *gcil-4*/13bl. However, the *gcil-4*/13bl gene sequence showed a large difference from that of *gcil-4/13b*, indicating that it is a new gene. Transcriptional expression analysis indicated that *il-4*/13bl was ubiquitously expressed in all examined tissues and significantly differed from g*cil-4/13b* expression profile. Functional studies showed that rgcIl-4/13bl prepared by prokaryotic expression system could activate HK M0/Mϕ with an evolutionarily conserved features. Further, rgcIl-4/13bl was able to promote the proliferation of M0/Mϕ derived from grass carp HK after rgcM-csf pretreatment. Taken together, our results reveal the conservation and diversity of the teleost *il-4/13* family, and enrich our knowledge of Il-4/13-mediated fish immunity.

2. Materials and methods

2.1. Fish

Healthy grass carp weighing about 750–1000 g were purchased from Chengdu Tongwei Aquatic Science and Technology Company (Chengdu, China). The fish were kept in aerated tap water at 20 ± 2 °C and acclimatized for two weeks before experiments. All experiments complied with the Regulation of Animal Use in Sichuan Province, China, and were approved by the ethics committee of the University of Electronic Science and Technology of China.

2.2. RNA isolation and cDNA synthesis

Grass carp tissues (~60 mg/ml) or cells (~2×10^6 cell/ml) were dissolved in Tripure Isolation Reagent (Roche, Basel, Switzerland) and the total RNA was isolated following the manufacturer's instruction. The first strand cDNA was synthesized using the M-MLV Reverse Transcriptase system (Promega, Madison, WI, USA) according to the manual and oligo $(dT)_{18}$ as the primer. The cDNA templates were used in molecular cloning and real-time quantitative PCR (qPCR) analysis.

2.3. Cloning of gcil-4/13bl CDS and gene sequence and analysis of gene structure

The mixture of the cDNAs from different tissues including gill, intestine, brain, thymus, skin, heart, head kidney and spleen was used as template to clone cDNA sequence of gcil-4/13bl. The partial CDS of *gcil-4*/13bl were obtained by PCR using High Fidelity Taq (NEB, MA, United Kingdom) and primers, *gcil-4*/13bl pF and pR (Supplementary Table 1) designed based on the conserved regions of *il-4/13b* sequences in other fishes. According to the partial sequence of *gcil-4*/13bl, the 5′- and 3′-sequences were obtained by 5′- and 3′-RACE System for Rapid Amplification of cDNA Ends kits (Thermo Scientific, Waltham, MA, USA), respectively, with gene-specific primers (Supplementary Table 1).

According to the cDNA sequence, we cloned *gcil-4*/13bl gene sequence using the pair of primers in 5′- and 3′- UTR, *gcil-4*/13bl UF and UR (Supplementary Table 1). Then, the 1600 bp-length fragment was ligated into pGEM-T vector (promega, Madison, WI, USA) and sequenced on ABI3730 Automated Sequencer (Applied Biosystem,USA) in Sangon Company (Chengdu, China). The homologues sequences of the other species were obtained from NCBI and the accession numbers were listed in Fig. 1. The aa sequence of grass carp Il-4/13a was from Ref. [7].

2.4. In silico analysis of gcil-4/13bl

The gene structure of *gcil-4*/13bl was analyzed by comparing CDS and gene sequence using two-sequence alignment program in BLAST (http://blast.ncbi.nlm.nih.gov/Blast.cgi). The aa sequence of gcIl-4/13bl was deduced using Translate tool in the ExPASy Molecular Biology server (http://web.expasy.org/translate/) and theoretical isoelectric point (pI) with molecular weight (MW) of deduced gcIl-4/13bl protein were calculated by Compute pI/MW in Expert Protein Analysis System (http://expasy.org/tools/). The signal peptide was predicted using the SignalP 4.1 (http://www.cbs.dtu.dk/services/SignalP/). N-glycosylation sites were predicted with NetNGlyc program. And a phylogenetic tree of *il-4/13* lineage genes was developed using MEGA v7.04 with Neibour-Joint method with the bootstrapping of 1000 repetitions [12] to obtain its evolutionary relationship. Similarity and identity at aa level were run with the program Matrix Global Alignment Tool (MatGAT) v2.0.3 [13]. Protein modeling was carried out using online software of Phyre2 (http://www.sbg.bio.ic.ac.uk/phyre2), and the server autosearched human IL-4 (d2b8ua1) as the best template for 3D modeling [14]. The key aa residues essential for binding to IL-4 receptor subunits were analyzed using models of mature peptides built by SWISS MODEL [15].

2.5. Tissue distribution of gcil-4/13b and gcil-4/13bl transcripts by qPCR analysis

Total RNA was extracted from organs included spleen, thymus, liver, heart, gill, intestine, brain, HK, muscle, skin and kidney. Total RNA was reverse-transcribed to cDNAs independently as described above and used as templates to quantitate the expression levels of *gcil-4*/13bl, *gcil-4/13b* and *β-actin* (the internal control) by qPCR. The gene-specific intron-spanning primers (Supplementary Table 1) were designed for qPCR. The qPCR was performed on a Bio-Rad CFX96 Real-time detection system (Bio-Rad, Hercules, CA, USA) in a final volume of 10 μl containing 5 μl of RealMasterMix (Tiangen, China), 1 μl of tissue cDNA as templates and 0.5 μl each of forward and reverse primer (10 μM). The qPCR program was 94 °C for 2 min, followed by 35 cycles of 94 °C for 20 s, 57 °C (*gcil-4*/13bl) or 60 °C (*gcβ-actin*) or 62 °C (*gcil-4/13b*) for 20 s and 65 °C for 30 s. A standard curve was generated for each target molecule by using the 10-fold serial dilutions (from 10^{-1} to 10^{-6} fmol) of plasmid containing the target gene sequence as template to evaluate the amplification efficiency. Parallel measurement of *β-actin* was conducted to serve as an internal control.

2.6. Recombinant expression and purification of rgcIl-4/13bl

The DNA fragment coding gcIl-4/13bl mature peptide (17–132 aa) was amplified by Phusion High-Fidelity DNA Polymerase (Thermo Scientific, Waltham, MA, USA) using primers rF and rR (Supplementary Table 1). The fragment was subcloned into pGEM-T easy (Promega, Madison, WI, USA) and then ligated into pET-30a (+) between BamHI and XhoI to obtain the recombinant plasmid of pET-30a (+)/gcIl-4/13bl. The positive clone was confirmed by sequencing and transformed into *E. coli* Rosetta-gami2 (DE3) (Merck Millipore, Billerica, MA, USA) for expression. Briefly, the induction was initiated by 1 mM isopropyl-β-D-thiogalactoside (IPTG, Merck, Darmstadt, Germany) at 30 °C for 6 h until the growth to an optical density at 600 (OD_{600}) of 0.6–0.8. The rgcIl-4/13bl protein was purified using HisTrap affinity columns (GE Healthcare, Waukesha, WI, USA) from the filtered supernatant of lysates and desalted by Superdex G200 prep grade columns (GE Healthcare). The molecular weight and purity of purified proteins were analyzed on SDS-PAGE. Bradford method was used to measure the concentration of target protein. The purified rgcIl-4/13bl protein was lyophilized and then stored at −80 °C for further use.

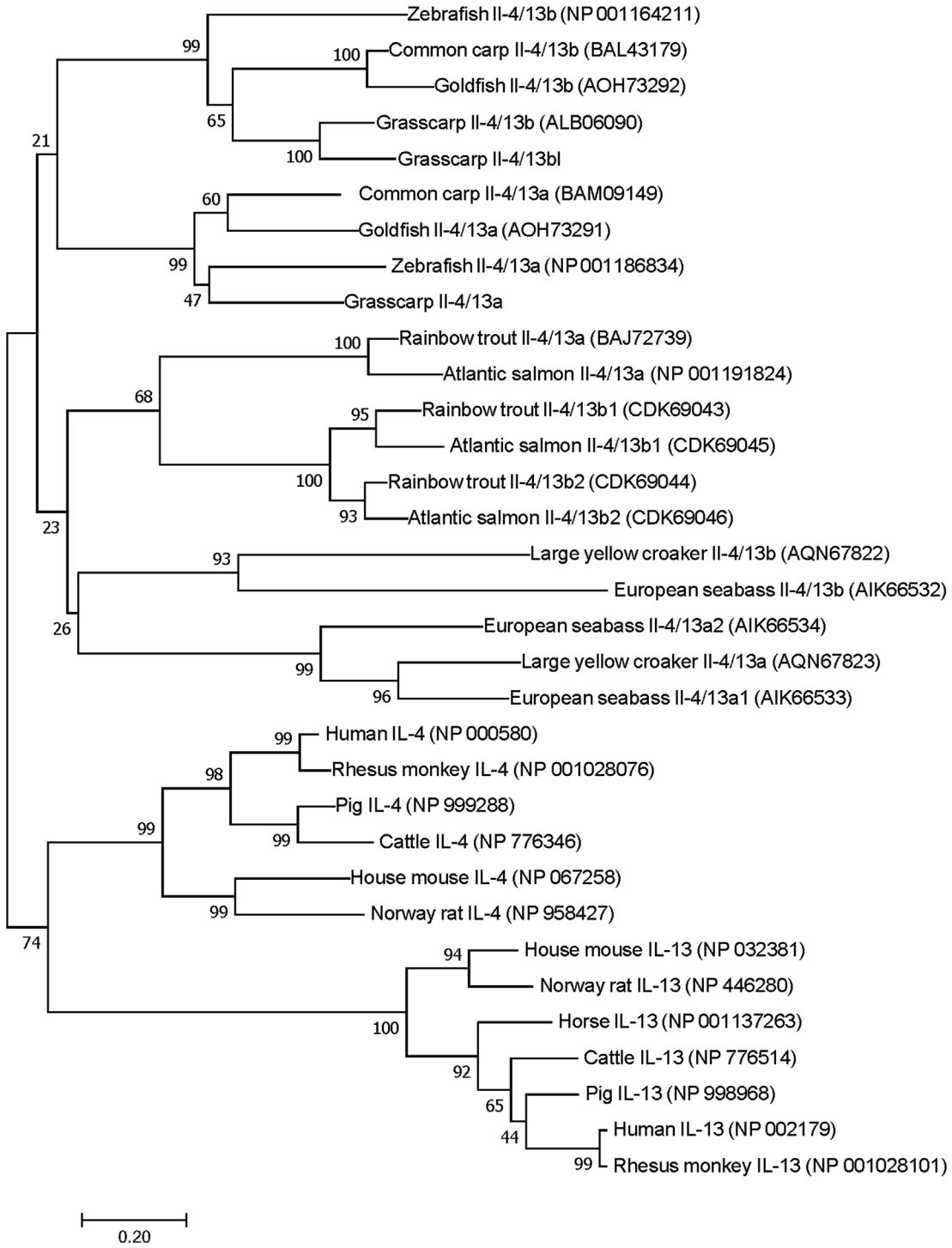

Fig. 1. Phylogenetic tree constructed based on fish IL-4/13 homologues and mammalian IL-4 and IL-13. Values at the forks indicate the frequency with which this grouping occurred after bootstrapping (1000 replicates). Scale bar shows number of substitutions per base. Accession numbers of the used sequences are shown in brackets.

2.7. Recombinant expression and purification of rgcM-CSF

The rgcM-csf protein was produced by *Pichia pastoris* system as before [16]. Briefly, extracellular region of gcM-csf1 (GenBank accession no.: MK548356, from position 29 to 202 aa) was constructed into pPICZαA with C-terminal 6 × his tag and transformed in X33 strain. The selected clone was cultured in 50 mL BMGY (1% yeast extract, 2% peptone, 100 mM potassium phosphate, 1.34% YNB, 4×10^{-5} biotin, 1% glycerol) at 29 °C with shaking at 250 rpm for approximately 12 h to the exponential growth. The cells were collected and resuspended with BMMY (1% yeast extract, 2% peptone, 100 mM potassium phosphate, 1.34% YNB, 4×10^{-5} biotin, 0.5% methanol, pH 4.0), and cultured in 100 ml BMMY at 29 °C with shaking at 250 rpm for approximately 48 h. The culture media were collected and purified by chromatography on a HisTrap affinity column (GE healthcare, Waukesha, WI, USA) and a Superdex G200 prep grade column (GE healthcare). The purified samples were analyzed by SDS-PAGE. Bradford method was used to measure the concentration of target protein. The purified rgcM-csf protein

was lyophilized and then stored at −80 °C for further use.

2.8. Isolation and culture of grass carp HK M0/Mϕ

Grass carp HK M0/Mϕ were prepared by discontinuous density gradient centrifugation using fish lymphocyte and monocyte preparation kit (TBD, Tianjin, China) [17]. In brief, HK was collected from freshly killed grass carp, washed twice and gently pressed in sample dilution buffer. The cell suspension was filtrated through a 200-gauge stainless steel mesh and was centrifuged at 400 × *g* for 25 min in a density gradient column formed by two solutions of different density. After that, M0/Mϕ enriched at the top layer of the separation solution and were collected. Cells were washed and resuspended in DMEM/F12 medium (pH 7.2, Life Technology) supplemented with 24 mM $NaHCO_3$, 25 mM HEPES, 1% antibiotic-antimycotic and incubated at 28 °C under 5% CO_2 and saturated humidity.

2.9. The qPCR analysis of marker genes's mRNA levels in grass carp HK M0/Mϕ

Grass carp HK M0/Mϕs were seeded at a density of 9×10^5/well in 48-well plate (BD Biosciences, San Jose, USA). On the following day, the floating cells were removed and the adherent cells were used for rgcIl-4/13bl treatment. These experiments were carried out as described in Section 2.5. The annealing temperatures for detection of *gcarg-1*, *gcarg-2*, *gcinos* and *gcifn-γ* mRNA were 62 °C, 57 °C, 60 °C and 63.5 °C, respectively. The mRNA level in control group was used to calibrate those in other groups.

2.10. Determination of nitric oxide (NO) production and arginase activity

Grass carp HK M0/Mϕs were isolated, seeded and treated as described in Section 2.8 and 2.9.

After treatment, the medium was analyzed for NO production using the Griess reaction [18]. Briefly, 75 μl culture medium was collected and incubated with 200 μl of Griess reagent (1% sulfanilamide, 0.1% naphthylethylene diamine dihydrochloride and 2.5% H_3PO_4) at room temperature for 15 min. The absorbance at 540 nm was detected in an iMark Microplate Absorbance Reader (Bio-rad). NO amount was determined using serially diluted sodium nitrite (Sigma) as a standard.

In the same wells, the cell cultures were washed and used for arginase activity measurement [19]. Cells were lysed in 50 μl of lysis buffer containing 0.1% Triton X-100, 5 μg pepstatin, 5 μg aprotinin and 5 μg antipain at room temperature for 30 min 50 μl of 10 mM $MnCl_2$ was added and the mixture was incubated for 10 min at 55 °C. To 50 μl of this activated lysate, 50 μl of 0.5 M L-arginine, pH 9.7 was added and incubated for 1 h at 37 °C. Reaction was stopped by adding 400 μl acid mixture containing H_2SO_4, H_3PO_4 and H_2O (1:3:7), then to each reaction 25 μl of 9% a-isonitrosopropiophenone (sigma, in 100% ethanol) was added and incubated for 45 min at 100 °C. After 10 min cooling in the dark the absorbance was read at 540 nm and arginase activity (mU = nmol urea formed per min) was calculated by comparison with a urea standard curve.

2.11. MTT assay

The freshly isolated HK M0/Mϕ were cultured in DMEM/F12, 10% fetal bovine serum (FBS), 2.5% grass carp serum and pre-treated with or without rgcM-csf (100 ng/ml) for about 5 days. Then, the cells were harvested and seeded in 96-well plate at a density of 10^5 cells/well in DMEM/F12 with 10% FBS at 26 °C. The cells were then treated with or without rgcIl-4/13bl (300 ng/ml) for the indicated time points. After treatment, 10 μl (5 mg/ml) 3-(4, 5-dimethylthiazol-2-yl)-2, 5-diphenyltetrazolium bromide (MTT) was added to each well for additional 4 h. The culture supernatant was then gently removed and the insoluble formazon salts produced were dissolved by adding 100 μl dimethyl sulfoxide (DMSO). Finally, the solvent was pippetted to a new 96-well plate for measuring the optical density value at 540 nm (OD_{540}) using microplate reader (BioRad). The medium of the same volumn without cells was set as blank, and the recordings from the blank were subtracted from the experimental groups. Three independent experiments were performed for this assay and the similar results were obtained.

2.12. Data analysis

Statistical analysis was conducted using one-way analysis of variance (ANOVA) followed by Fisher's least significant difference (LSD) tests using SPSS13.0 software. For comparison between two groups, Student's t-test was used. Differences were considered as significant at $p < 0.05$. At least three individual experiments were conducted and the representative results were presented.

3. Results

3.1. Molecular cloning and sequence analysis of gcil-4/13bl

A new *il-4/13* cDNA was cloned from grass carp via homology cloning (GenBank accession no.: MK548354). The cDNA sequence is 559 bp in length and contains a CDS of 399 nt, which is predicted to encode a 132-aa polypeptide with a calculated molecular weight (MW) of 15.1 kDa. A putative signal peptide is 1–16 aa from the N terminus. The phylogenetic tree showed that the new *il-4/13* clustered with *gcil-4/13b* (Fig. 1), which was consistent with the multiple alignment results in which the aa sequence of the new *il-4/13* was closer to *gcIl-4/13b* (74.1%) than to *gcIl-4/13a* (23.9%) (Table 1). Thus, it was nominated as *gcil-4*/13bl in order to distinguish *gcil-4/13b* obtained from transcriptome data of grass carp peritoneal cells by using a BLAST search [7]. The sequence alignments between *gcil-4/13b* and *gcil-4*/13bl showed that scattered variations located all over the whole nucleotide acid sequence (Fig. S1A). The large differences appeared in α-helix A and C where three adjacent amino residues (YAD) existed in gcIl-4/13b but not gcIl-4/13bl (Fig. S1B). Furthermore, the 3D models displayed that the complete α-helix C in gcIl-4/13b was split into two pieces in gcIl-4/13bl (Fig. S1C).

3.2. Gene structure analysis

To examine whether *gcil-4*/13bl is derived from another locus distinct from *gcil-4/13b*, we cloned and screened the *gcil-4*/13bl gene sequence as mentioned in Materials and methods, and a band of 1600 bp in length was obtained (GenBank accession no.: MK548355). The CDS and the gene sequence were aligned by using BLAST in NCBI. It revealed that the 1600 bp-length sequence was the gene for *gcil-4*/13bl which was longer than that of *gcil-4/13b* (900 bp). As shown in Fig. S2, *gcil-4*/13bl gene sequence was composed of four exons and three introns, which is conserved through all known fish *il-4/13* and mammalian *IL-4* and *IL-13* homologues (Fig. 2). Moreover, *gcil-4*/13bl gene harbored a longer intron 3 sequence (951 bp) than *gcil-4/13b* (297 bp), which is similar with fish *il-4/13b* and other species *IL-4* counterparts (human, 2598 bp; mouse, 1285 bp; Xenopus, 2044 bp) (Fig. 2).

3.3. Tissue distribution

We designed the gene-specific primers to distinguish *gcil-4/13b* and *gcil-4*/13bl by qPCR. In healthy fish individuals, the transcripts of *gcil-4/13b* were detected with the highest level in gill and skin, and the lowest level in brain and HK. While *gcil-4*/13bl constitutively expressed in all tissues tested by qPCR with the highest level in gill, to a lesser extent in skin and intestine and other tissues (liver, brain, thymus, HK and heart), while the lowest level in muscle. Moreover, the transcript levels of *gcil-4*/13bl were generally lower than that of *gcil-4/13b* in other selected tissues, but higher by 70 and 8 folds than that of *gcil-4/*

Table 1
The identity of gcIl-4/13bl aa sequence with their homologues in other vertebrates. The same numbers in the first row and column represent the species in the list. The numbers in the upper right panel with the light grey background represent the identity. The numbers in the lower left panel with blank background represent the similarity. The accession numbers in GeneBank are listed in Fig. 1.

	1	2	3	4	5	6	7	8	9	10	11	12	13	14	15	16	17	18	19	20	21	22	23	24
1. Grass carp Il-4/13a		25.7	23.9	25.4	42.7	51.4	30.2	48.6	26.4	27.9	27.1	27.1	26.1	22.4	23.8	21.5	23.4	19.6	24.3	22.5	20.7	15.3	25	17.2
2. Grass carp Il-4/13b	49.6		74.1	39.7	25.5	27.6	46.7	27.2	43.5	23.4	27.5	22.9	25	27.2	26.8	19.6	22	20.4	18.9	19	20.5	17.4	22.3	17.5
3. Grass carp Il-4/13bl	45.9	82.2		38.3	27.5	23.1	42.2	24.1	44.2	21.4	24.7	21.6	21.6	25.3	23	20.9	25.8	19.7	21.8	20.3	21.2	20	23.9	14.5
4. Zebrafish Il-4/13b	40.6	54.1	55.3		22.8	25.4	45.3	21.7	38.2	18.4	20.4	27.3	16.7	19.1	24.3	21.9	19.1	18.1	20.4	18	22.4	12.7	21.3	15.4
5. Zebrafish Il-4/13a	57.3	43.3	43.9	35.7		45.9	24.1	42	21	28	22.2	22.9	24.7	21.8	25.2	20.9	22.2	19.1	21.5	16.4	18.5	18.1	19.6	21.1
6. Common carp Il-4/13a	65.2	45.9	45.2	35.6	58.6		21	65	20.5	27.3	30.1	31.8	25.3	26.1	31.4	24.7	21.6	20.8	22.4	17.6	19.4	22.1	25.3	21
7. Common carp Il-4/13b	40.6	63.7	64.4	60.6	38.9	41.5		21.6	80	19.6	20.7	23.3	22.7	20.5	22.7	20.4	17.3	21.8	21.7	16.4	17.9	12.9	23.1	16
8. Goldfish Il-4/13a	64.2	41.6	44.5	39.4	57.3	78.1	38		21.1	26.8	27.9	28.8	22.9	27.6	28.1	22.5	20.4	23.3	25.5	18.8	17.5	19.3	22.7	20
9. Goldfish Il-4/13b	43	62.2	63	53.3	37.6	42.2	86.7	40.1		19.1	19.9	22.1	19.3	19.2	22.7	19.9	17.8	20.8	23.2	14.5	15.5	15.3	20.5	19.1
10. Rainbow trout Il-4/13a	44.1	41.4	42.8	33.1	47.8	47.6	35.9	44.8	37.9		27.6	24.1	81.5	27	27.9	25.9	23	26.5	27	26	17.9	17.3	24.1	18.2
11. Rainbow trout Il-4/13b1	38.7	43.3	41.3	35.3	37.6	43.3	34	40.7	33.3	42.7		66	24.1	82	65.1	24.1	23	17.7	15.8	16.5	18.5	16.2	17.9	14.4
12. Rainbow trout Il-4/13b2	35.9	37.3	38.6	38.6	40.1	47.1	37.9	43.8	34.6	41.2	75.8		26.1	62.7	82.4	16.3	22.8	21.4	16.9	18.3	17	20.9	20.4	15
13. Atlantic salmon Il-4/13a	43.7	45.1	45.1	33.8	43.9	49.3	43.7	44.4	43	89	42	41.8		24.1	26.5	25.9	23.5	22.7	24.5	28.4	18.2	16.6	21.6	18.8
14. Atlantic salmon Il-4/13b	37.3	44	42.7	32	39.5	41.3	35.3	40.7	34	44.7	88	72.5	44		61.8	16.1	21.2	22.5	14.5	18.8	17.3	18.1	13.5	14.4
15. Atlantic salmon Il-4/13b	33.3	40.8	40.1	38.8	42	46.3	37.4	42.2	33.3	45.6	74.7	86.3	44.9	72.7		19.7	18	20.4	17.6	20	20.9	19.1	22.8	18.3
16. Large yellow croaker Il-4/13a	43.9	41.2	43.9	33.8	41.4	45.3	39.2	39.9	39.2	44.6	42	34.6	43.9	35.3	37.2		19.9	52.3	40	20.2	13.4	18.7	16.4	12.8
17. Large yellow croaker Il-4/13a	42.3	37.8	41.7	36.5	47.1	43.6	35.9	41	35.9	40.4	39.1	41.7	37.8	39.7	34.6	37.8		15.4	20.4	31.9	17.5	19.1	14.7	14.5
18. European seabass Il-4/13a1	43.1	38.9	44.4	32.6	41.4	43.8	36.8	43.1	41.7	44.1	34	35.3	44.4	41.3	40.8	71.6	39.7		37.9	16.4	13.7	16.4	18.4	15.8
19. European seabass Il-4/13a2	46.5	37.3	42.3	34.5	39.5	45.1	40.1	45.8	40.1	45.5	32	35.3	45.8	34	29.9	57.4	41.7	59		20.6	17.7	21.6	18.7	15.9
20. European seabass Il-4/13b	40.5	33.1	40.5	33.8	43.9	39.9	36.5	39.9	40.5	40.5	40.7	41.2	45.3	42	39.2	40.5	53.2	37.8	36.5		14.1	18.7	18.5	16.2
21. House mouse IL-4	42.1	42.1	46.4	43.6	33.1	38.6	37.9	36.4	34.3	31.7	33.3	34	34.5	30.7	34	30.4	34	31.9	36.6	31.1		18.9	40.3	20.4
22. House mouse IL-13	30.8	31.1	39.4	28.2	35.7	38.5	38.2	36.5	38.5	33.8	32	37.9	35.9	31.3	36.1	30.4	32.7	38.2	37.3	31.8	33.6		18.6	52.7
23. Human IL-4	41.8	41.8	41.2	37.3	37.6	39.9	38.6	39.2	35.9	39.9	32	35.3	39.2	30.7	34	34	37.2	35.3	34.6	34.6	56.9	37.9		22.4
24. Human IL-13	34.9	34.2	29.5	28.1	42	39.7	33.6	42.5	35.6	36.3	27.3	28.1	37	28	32	35.8	34.6	37	31.5	33.8	39	65.8	36.6	

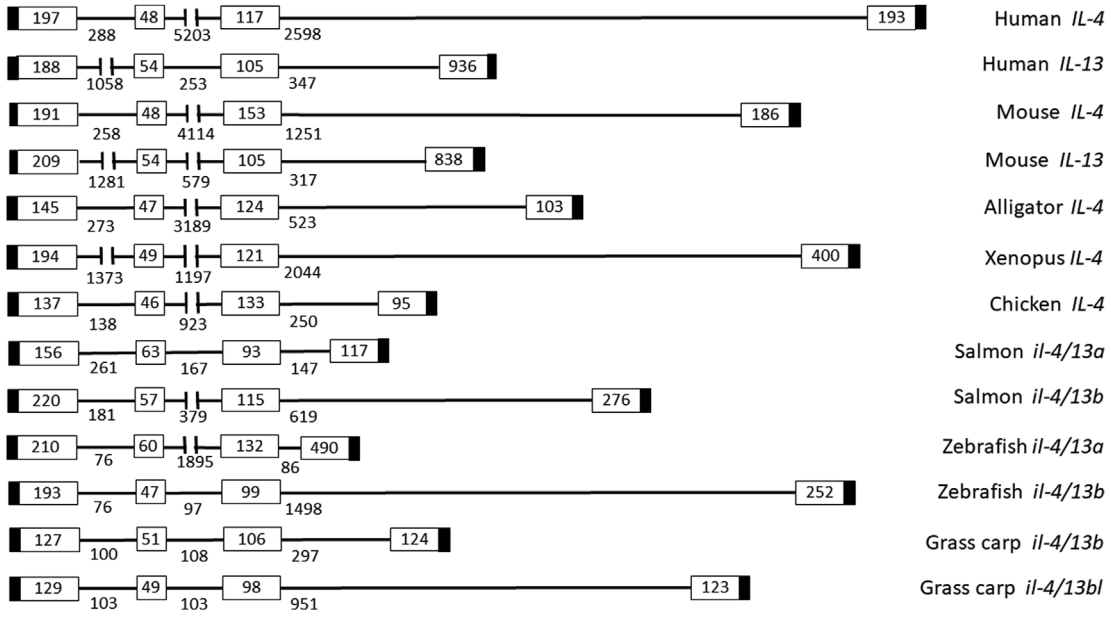

Fig. 2. The diagram of gene structure of mammalian IL-4, IL-13 and fish Il-4/13 homologues. The blank rectangles represent exons and the numbers indicate the length. The black rectangles represent 5′- and 3′-UTRs. The lines between the rectangles indicate introns and the numbers below reveal the length. The lines of intron 3 are scaled to their length.

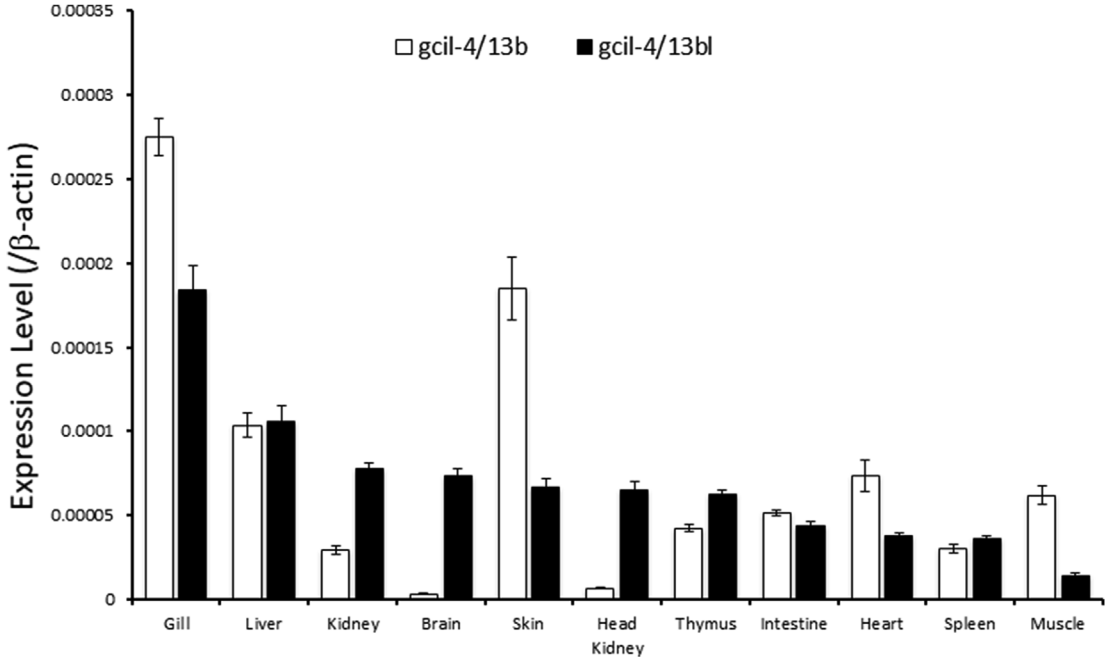

Fig. 3. Expression pattern of *gcil-4/13b* and *gcil-4*/13bl. Total RNAs were extracted from the selected tissues. The mRNA expression levels of *gcil-4/13b* and *gcil-4*/13bl were quantified by qPCR. The mRNA levels of *gcil-4/13b* and *gcil-4*/13bl were normalized by β-actin in the same samples. Data presented are expressed as mean ± SEM (N = 6).

13b in brain and HK (Fig. 3).

3.4. Effect of rgcIl-4/13bl on alternatively activation of HK M0/Mϕ

In order to assess the bioactivity of gcIl-4/13bl, we prepared and purified rgcIl-4/13bl using *E. coli* strain Rosetta-gami 2 (DE3). SDS-PAGE analysis showed that the purity of rgcIl-4/13bl (18.8 kDa) reached more than 95% (Fig. S3). Subsequently, the effects of rgcIl-4/13bl on the arginase activity and NO production from freshly isolated HK M0/Mϕ were detected. The results showed that the arginase activity was upregulated in a dose-dependent manner, reaching the highest level at the dose of 300–1000 ng/ml ranged from 6 to 24 h. Whereas NO production from the same cultures was inhibited by 15% at the same doses after 24-h treatment (Fig. 4). Furthermore, the transcript levels of *inos*, *arginase 1*, *arginase 2* and *ifn*-γ were examined, showing that rgcIl-4/13bl was able to upregulate *arginase 2* but not *arginase 1* mRNA expression at 6- and 24-h treatment. Conversely, the mRNA levels of *inos* and *ifn*-γ were inhibited by 30% and 40%, respectively (Fig. 5). Meanwhile, the heat inactive rgcIl-4/13bl (1000 ng/ml) did not alter the arginase activity, NO production and the mRNA expression of the detected genes.

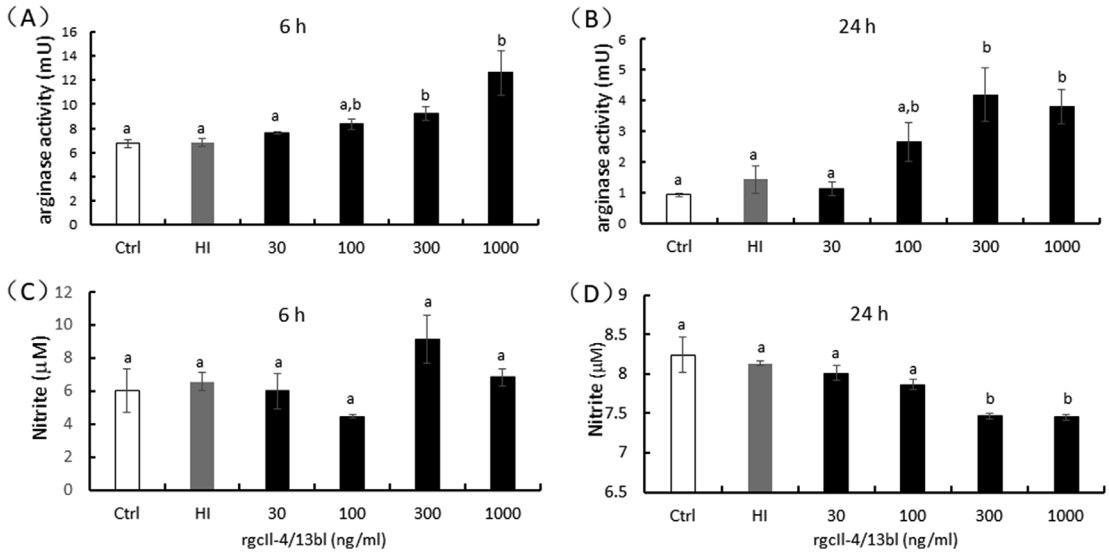

Fig. 4. Effect of rgcIl-4/13bl on arginase activity and NO production in grass carp M0/Mϕ. Cells, 5×10^5 per well, were treated with the increasing doses (30–1000 ng/ml)of rgcIl-4/13bl for 6 h (A and C) or 24 h (B and D). Then the cells were collected to detect arginase activity (A and B) while the media from the same wells were used for NO production assay (C and D). rgcIl-4/13bl (1000 ng/ml) was heated for 30 min at 90 °C and used as the heat-inactive (HI) protein. Data presented are expressed as mean ± SEM (N = 4). The different letters indicate the statistically significant differences ($p < 0.05$).

3.5. Effect of rgcIl-4/13bl on the proliferation of M0/Mϕ pre-treated by rgcM-csf

Firstly, we prepared rgcM-csf using *Pichia pastrios* expressing system. The purified protein has a MW of approximately 36 kDa (Fig. S4) which is bigger than that of the predicted rgcM-csf fusion protein (26 kDa). Subsequently, HK M0/Mϕ were cultured in the absence or presence of rgcM-csf (100 ng/ml) for 5 days. After removal of the floating cells, the adherent cells and cell clusters were collected and washed. The same number of cells were seeded in each wells and treated by rgcIl-4/13bl alone or not for the indicated time points. The flow chat of the experiment was shown in Fig. 6A. The cell proliferation in these groups was examined by MTT assay. As shown in Fig. 6B, compared with Ctrl group, the OD_{540} values increased in a time-dependent manner from 48 h and peaked at 96 h by about 18 folds in group treated by rgcIl-4/13bl alone (rgcIl-4/13bl vs Ctrl). RgcIl-4/13bl was also able to boost a time-dependent enhancement in OD_{540} value from 24 h in group pre-treated by rgcM-csf (rgcM-csf + rgcIl4/13bl vs rgcM-csf), with the peak response by 32 folds noted at 96 h.

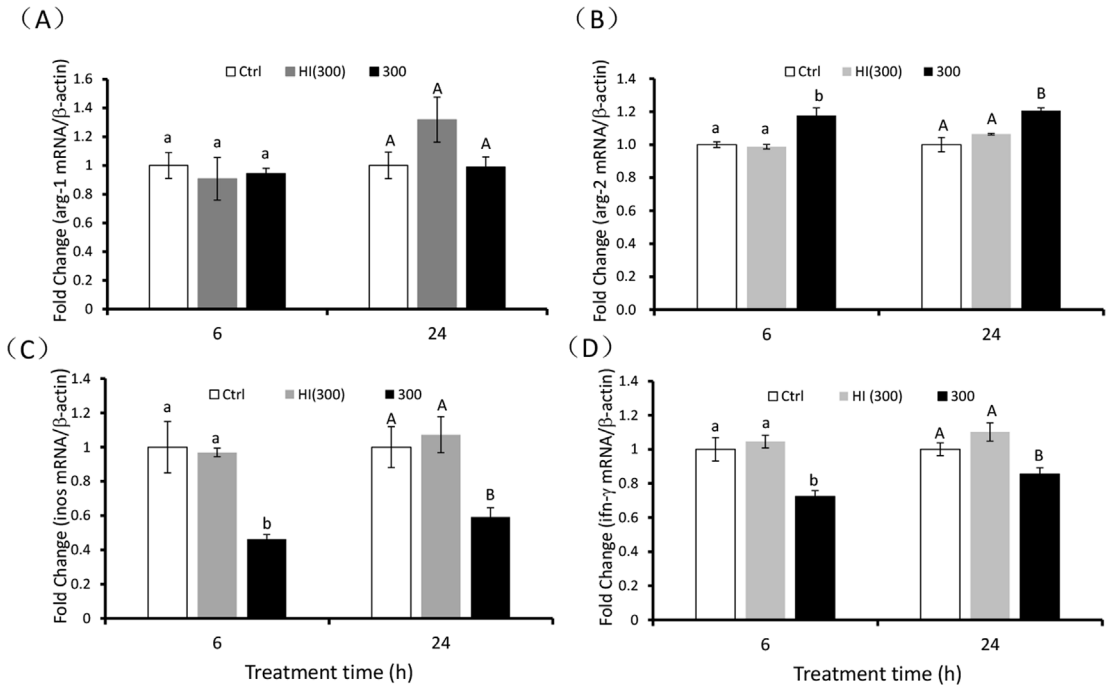

Fig. 5. Effect of rgcIL-4/13bl on *arginase-1* (A), *arginase-2* (B), *inos* (C) and *ifn*-γ (D) transcript levels in grass carp M0/Mϕ. Grass carp M0/Mϕ were treated with rgcIl-4/13bl (300 ng/ml) for 6 and 24 h rgcIl-4/13bl (300 ng/ml) was heated for 30 min at 90 °C and used as the heat-inactive (HI) protein. The mRNA levels of arginase-1, arginase-2, inos and ifn-γ were detected by qPCR and normalized by β-actin. The expression as fold changes compared with the control groups is shown. Data presented are expressed as mean ± SEM (N = 4). The different letters denote significant differences ($p < 0.05$).

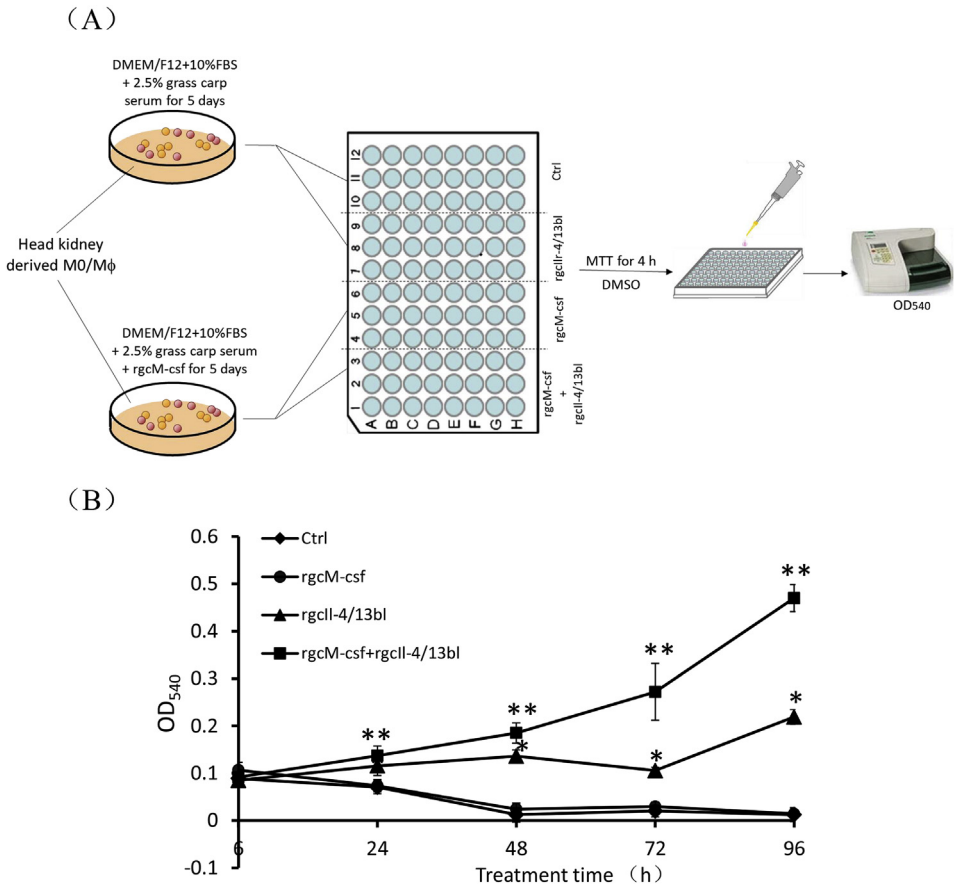

Fig. 6. Cell proliferation of M0/Mϕ in the presence or absence of rgcM-csf (100 ng/ml) and/or rgcIl-4/13bl (300 ng/ml). (A) The flow chart of the experiments. There individual experiments were conducted as mentioned in "Materials and Methods" (2.10 MTT assay). (B) The MTT assay was used to determine the cell viability after rgcIl-4/13bl treatment for the indicated time points and the OD_{540} (vertical bar) was shown. Bars are presented as mean ± SEM (N = 6). The asterisks (*) denote significant differences at $p < 0.05$ relative to the time-matched controls. The double asterisks (**) indicate significant differences at $p < 0.01$ relative to the groups just pre-treated by rgcM-csf.

4. Discussion

Recently, two more loci of *il-4*/13 has been identified in both Atlantic salmon and rainbow trout, two 4 round whole genome dupliation (4R WGD) species, indicating that fish *il-4/13* family is composed of multigenes [9]. In the present study, CDS sequences variations (Fig. S1A &B) and the difference between gene structures of *gcil-4/13b* and *gcil-4*/13bl (Fig. 2) revealed the existence of the third locus of *il-4/13* in addition to *gcil-4/13a* and *gcil-4/13b* in grass carp genome. Besides, the helix A and C, which are proposed to form "AC face", essential for ligand-receptor binding in mammals [20], were largely different between *gcil-4/13b* and *gcil-4*/13bl (Fig. S1C). Especially, *gcil-4/13b* possess a complete helix C, but in *gcil-4*/13bl, helix C was divided into two pieces due to the lack of three amino acid (YAD) residues (Fig. S1C). Thus, it is required to investigate the function of the newly cloned *gcil-4*/13bl.

The sequence analysis uncovered that two mRNA destabilization motifs (ATTTA) and one poly-adenylation motif (ATAAAAA) presented in *gcil-4*/13bl cDNA sequence (Fig. S2), suggesting an active transcription status of *gcil-4*/13bl. Tissue distribution assay revealed that *gcil-4*/13bl mRNA were detected in almost all tissues, which is consistent with the tissue distribution patterns of green-spotted puffer *il-4/13a* [5], zebrafish *il-4/13a* [21], and large yellow croaker *il-4/13b* [11], suggesting its broad roles in organs. It was worth mentioning that the transcripts of *gcil-4*/13bl were lower than that of *gcil-4/13b* in tissues except brain and HK (Fig. 3). The role of gcIl-4/13bl in fish brain is unknown, but the study in human brain may give us some inspiration in which IL-4 is capable of inducing microglia, the resident macrophage in brain, into M2-type macrophage [22,23]. HK is fish unique organ, and recognized as the equivalent of mammalian bone marrow [24]. The immunohistochemical study demonstrates that macrophages appear from day 2 post-fertilization in HK, allowing an early non-specific defense in young fish [25]. More recently, bony fish macrophages biology and polarization have attracted the increasing attentions mainly in view of their roles in host protection and homeostasis due to their widespread in virtually all tissues [26,27]. All of these led us to explore the functional role of gcIl-4/13bl in macrophages.

Similar to mammals, fish also have polarization patterns of M1-and M2-type macrophages [28]. In our previous study, rgcIfn-γ is able to enhance NO production and proinflammatory cytokines Il-1β and Tnf-α in primary HK M0/Mϕ, which showed a classical activation status of macrophages (M1) [17]. In this study, the addition of rgcIl-4/13bl upregulated arginase activity in a dose- and time-dependent manner (Fig. 4). In later phase, it inhibited NO production in the freshly isolated M0/Mϕ from HK (Fig. 4). This tendency was reinforced by the results that the gene expression of *arginase-2* was enhanced, while the transcripts levels of grass carp *inos* and *ifn*-γ were attenuated (Fig. 5), as seen in the other fish species counterparts [10,11]. Accordingly, despite the dissimilarities in tertiary structures compared with gcIl-4/13b, gcIl-4/13bl performed the evolutionarily conserved function in promoting M2-type while antagonizing M1-type macrophages.

Mammalian IL-4 can promote macrophages proliferation. IL-4-driven rapid *in situ* expansion of tissue macrophages may prevent inflammatory cell recruitment and the associated potential for tissue damage [29]. In this study, the cell numbers were counted using Hausser Bright-Line counting chamber after rgcIl-4/13bl treatment for 24 h, finding that the viable cell numbers were obviously enhanced by rgcIl-4/13bl, especially in the groups which were pre-treated by rgcM-csf (Data not shown). Furthermore, MTT assay was conducted, and the results showed significant cell proliferation driven by rgcIl-4/13bl, reflected by the increase of OD_{540} from 6 to 96 h in rgcIl-4/13bl treated groups (Fig. 6B). Moreover, rgcIl-4/13bl promoted even faster proliferation in rgcM-csf pre-treated group than that without rgcM-csf pretreatment (Fig. 6B). In mammals, IL-4 often promotes tumor associated

macrophages (TAM) cell proliferation combined with M-CSF [30]. Given that recombinant goldfish M-csf can differentiate monocytes into macrophages [31], we suggest that gcIl4/13bl might promote macrophage proliferation after M-csf induced cell differentiation in fish.

Recently, several studies have shown that fish Il-4/13a and Il-4/13b have similar functions in alternatively activating monocytes/macrophages [7, 10, 11]. And in the present study, the newly identified gcIl-4/13bl, was also shown to be able to perform the same function with its two paralogues, gcIl-4/13a and gcIl-4/13b. Further, we wonder if gcIl-4/13a and gcIl-4/13b play the same role in promoting cell proliferation as gcIl-4/13bl. Thus, their abilities to bind different receptor subunits were compared through the key aa residues according to studies on human and mouse IL-4 ligand-receptor binding [20] predicted by homology modeling using SWISS MODEL [15]. As shown in Supplementary Table 2, the key aa residues were all conserved in human and mouse IL-4 and their counterparts in grass carp, indicating that the family homologues might all be able to perform the similar function.

5. Conclusions

Collectively, we identified a new protein-coding locus of *il-4/13* in grass carp via homology cloning. Our data showed that the multigene family of *il-4/13* existed in fish species beyond 4R WGD-derivative salmonid fishes. These results also show macrophage proliferation driven by IL-4 in mammals can be traced to teleost fish. All of these revealed the multiple functions of Il-4/13 in regulating M0/Mϕ, and will enhance our understanding in the roles of Il-4/13 in fish.

Acknowledgements

This work was supported by the National Natural Science Foundation of China under Grants 31602192 and Fundamental Research Funds for the Central Universities in UESTC under Grant ZYGX2015J090.

Appendix A. Supplementary data

Supplementary data to this article can be found online at https://doi.org/10.1016/j.fsi.2019.07.070.

Table 1 The identity of gcIl-4/13bl aa sequence with their homologues in other vertebrates. The same numbers in the first row and column represent the species in the list. The numbers in the upper right panel with the light grey background represent the identity. The numbers in the lower left panel with blank background represent the similarity. The accession numbers in GeneBank are listed in Fig. 1.

References

[1] D.A. Rozwarski, A.M. Gronenborn, G.M. Clore, J.F. Bazan, A. Bohm, A. Wlodawer, et al., Structural comparisons among the short-chain helical cytokines, Structure 2 (1994) 159–173.
[2] T. Wang, C.J. Secombes, The evolution of IL-4 and IL-13 and their receptor subunits, Cytokine 75 (2015) 8–13.
[3] L.B. Bacharier, H. Jabara, R.S. Geha, Molecular mechanisms of immunoglobulin E regulation, Int. Arch. Allergy Immunol. 115 (1998) 257–269.
[4] P.R. Taylor, S. Gordon, Monocyte heterogeneity and innate immunity, Immunity 19 (2003) 2–4.
[5] J.H. Li, J.Z. Shao, L.X. Xiang, Y. Wen, Cloning, characterization and expression analysis of pufferfish interleukin-4 cDNA: the first evidence of Th2-type cytokine in fish, Mol. Immunol. 44 (2007) 2078–2086.
[6] M. Ohtani, N. Hayashi, K. Hashimoto, T. Nakanishi, J.M. Dijkstra, Comprehensive clarification of two paralogous interleukin 4/13 loci in teleost fish, Immunogenetics 60 (2008) 383–397.
[7] Z.J. Yang, C.H. Li, J. Chen, H. Zhang, M.Y. Li, J. Chen, Molecular characterization of an interleukin-4/13B homolog in grass carp (Ctenopharyngodon idella) and its role in fish against Aeromonas hydrophila infection, Fish Shellfish Immunol. 57 (2016) 136–147.
[8] G. Biswas, R. Nagamine, J.I. Hikima, M. Sakai, T. Kono, Inductive immune responses in the Japanese pufferfish (Takifugu rubripes) treated with recombinant IFN-gamma, IFN-gammarel, IL-4/13A and IL-4/13B, Int. Immunopharmacol. 31 (2015) 50–56.
[9] T. Wang, P. Johansson, B. Abos, A. Holt, C. Tafalla, Y. Jiang, et al., First in-depth analysis of the novel Th2-type cytokines in salmonid fish reveals distinct patterns of expression and modulation but overlapping bioactivities, Oncotarget 7 (2016) 10917–10946.
[10] J.W. Hodgkinson, C. Fibke, M. Belosevic, Recombinant IL-4/13A and IL-4/13B induce arginase activity and down-regulate nitric oxide response of primary goldfish (Carassius auratus L.) macrophages, Dev. Comp. Immunol. 67 (2017) 377–384.
[11] K. Mao, W. Chen, Y. Mu, J. Ao, X. Chen, Identification of two IL-4/13 homologues in large yellow croaker (Larimichthys crocea) revealed their similar roles in inducing alternative activation of monocytes/macrophages, Fish Shellfish Immunol. 80 (2018) 180–190.
[12] S. Kumar, G. Stecher, K. Tamura, MEGA7: molecular evolutionary genetics analysis version 7.0 for bigger datasets, Mol. Biol. Evol. 33 (2016) 1870–1874.
[13] J.J. Campanella, L. Bitincka, J. Smalley, MatGAT: an application that generates similarity/identity matrices using protein or DNA sequences, BMC Bioinf. 4 (2003) 29.
[14] L.A. Kelley, S. Mezulis, C.M. Yates, M.N. Wass, M.J.E. Sternberg, The Phyre2 web portal for protein modeling, prediction and analysis, Nat. Protoc. 10 (2015) 845.
[15] A. Waterhouse, M. Bertoni, S. Bienert, G. Studer, G. Tauriello, R. Gumienny, et al., SWISS-MODEL: homology modelling of protein structures and complexes, Nucleic Acids Res. 46 (2018) W296–w303.
[16] K. Yang, Separation, Identification and a Novel Activation Mechanism of Grass Carp Headkidney Monocytes/macrophages, University of Electronic Science and Technology of China, 2014.
[17] K. Yang, S. Zhang, D. Chen, A. Zhang, X. Wang, H. Zhou, IFN-γ-activated lymphocytes boost nitric oxide production in grass carp monocytes/macrophages, Fish Shellfish Immunol. 35 (2013) 1635–1641.
[18] L.C. Green, D.A. Wagner, J. Glogowski, P.L. Skipper, J.S. Wishnok, S.R. Tannenbaum, Analysis of nitrate, nitrite, and [15N]nitrate in biological fluids, Anal. Biochem. 126 (1982) 131–138.
[19] I. Corraliza, M. Campo, G. Soler, M. Modolell, Determination of arginase activity in macrophages: a micromethod, J. Immunol. Methods 174 (1994) 231–235.
[20] T.D. Mueller, J.L. Zhang, W. Sebald, A. Duschl, Structure, binding, and antagonists in the IL-4/IL-13 receptor system, Biochim. Biophys. Acta 1592 (2002) 237–250.
[21] L.Y. Zhu, P.P. Pan, W. Fang, J.Z. Shao, L.X. Xiang, Essential role of IL-4 and IL-4Ralpha interaction in adaptive immunity of zebrafish: insight into the origin of Th2-like regulatory mechanism in ancient vertebrates, J. Immunol. 188 (2012) 5571–5584.
[22] X. Liu, J. Liu, S. Zhao, H. Zhang, W. Cai, M. Cai, et al., Interleukin-4 is essential for microglia/macrophage M2 polarization and long-term recovery after cerebral ischemia, Stroke Cereb. Circ. 47 (2016) 498.
[23] S.P. Gadani, J.C. Cronk, G.T. Norris, J. Kipnis, IL-4 in the brain: a cytokine to remember, J. Immunol. 189 (2012) 4213–4219.
[24] M. Joerink, C.M. Ribeiro, R.J. Stet, T. Hermsen, H.F. Savelkoul, G.F. Wiegertjes, Head kidney-derived macrophages of common carp (Cyprinus carpio L.) show plasticity and functional polarization upon differential stimulation, J. Immunol. 177 (2006) 61–69.
[25] P.C. Hanington, J. Tam, B.A. Katzenback, S.J. Hitchen, D.R. Barreda, M. Belosevic, Development of macrophages of cyprinid fish, Dev. Comp. Immunol. 33 (2009) 411–429.
[26] J.W. Hodgkinson, L. Grayfer, M. Belosevic, Biology of bony fish macrophages, Biology 4 (2015) 881–906.
[27] G.F. Wiegertjes, A.S. Wentzel, H.P. Spaink, P.M. Elks, I.R. Fink, Polarization of immune responses in fish: the 'macrophages first' point of view, Mol. Immunol. 69 (2016) 146–156.
[28] M. Joerink, H.F. Savelkoul, G.F. Wiegertjes, Evolutionary conservation of alternative activation of macrophages: structural and functional characterization of arginase 1 and 2 in carp (Cyprinus carpio L.), Mol. Immunol. 43 (2006) 1116–1128.
[29] S.J. Jenkins, D. Ruckerl, P.C. Cook, L.H. Jones, F.D. Finkelman, N. van Rooijen, et al., Local macrophage proliferation, rather than recruitment from the blood, is a signature of TH2 inflammation, Science 332 (2011) 1284–1288.
[30] H.W. Wang, J.A. Joyce, Alternative activation of tumor-associated macrophages by IL-4, Cell Cycle 9 (2010) 4824–4835.
[31] P.C. Hanington, S.J. Hitchen, L.A. Beamish, M. Belosevic, Macrophage colony stimulating factor (CSF-1) is a central growth factor of goldfish macrophages, Fish Shellfish Immunol. 26 (2009) 1–9.